

## Equilibrium Swelling of Hydrophilic Polyacrylates in Humid Environments

Wan-Lin Chen<sup>†</sup> and Kenneth R. Shull<sup>\*,‡</sup>

*Department of Chemical Engineering and Department of Materials Science and Engineering, Northwestern University, 2225 North Campus Drive, Evanston, Illinois 60208-3108*

Theodore Papatheodorou, Dmitrii A. Styckas, and Joseph L. Keddie

*School of Physical Sciences, University of Surrey, Guildford GU2 5XH, UK*

*Received August 25, 1998; Revised Manuscript Received November 6, 1998*

**ABSTRACT:** The hydrophilicity of polymers, as indicated by their swelling characteristics in water, is an important parameter with regard to their use as coatings which are able to modify the wettability and adhesive properties of a material. We have investigated the swelling behavior of a series of hydrophilic random copolymer coatings in controlled humidity environments and in water. Swelling data were obtained from a quartz crystal microbalance (QCM) and from spectroscopic ellipsometry. The hydrophilic polymers are based on polyacrylates with low molecular weight side chains of poly(ethylene glycol) (PEG). These polymers also contain a random distribution of acrylic acid. Triblock copolymers with these random copolymers as the midblock and poly(methyl methacrylate) (PMMA) as the end blocks have also been investigated. At low and intermediate humidities, the swelling behavior of appropriately chosen block copolymers is similar to the swelling behavior of the corresponding polymers that do not have the PMMA end blocks. Substantial differences between the two types of polymers are observed at very high humidities and in water. The PMMA end blocks stabilize the structure of the copolymer layer so that it does not dissolve in water. Swelling curves obtained from the quartz crystal microbalance and from ellipsometry are in agreement with one another when the shape of the quartz crystal resonance (as determined by impedance spectroscopy) is not affected by humidity. We also find evidence for a reversible, humidity-induced phase transition which is readily detectable by the quartz crystal microbalance.

### Introduction

A variety of reasons exist to apply hydrophilic coatings to the surface of a material. Often, the goal is to enhance the adhesion or wettability of the surface so that other coatings (such as paint) can be effectively applied.<sup>1,2</sup> In other cases the goal is to minimize adhesion, as with antifouling coatings designed to reduce the adhesion of biological organisms.<sup>3,4</sup> Hydrophilic surfaces have been obtained by a variety of methods, including plasma polymerizations of water-soluble polymers,<sup>5</sup> chemical reactions to introduce polar functional groups,<sup>6</sup> and surface processing to coat hydrophilic polymers on surfaces.<sup>4</sup> Our focus is on the development of hydrophilic coatings that can easily be applied to a variety of surfaces with standard coating techniques. Here the swelling behavior of the coating serves as a useful measure of the hydrophilic character of the surface.

Because the hydrophilic coatings can be quite thin, any technique for studying their swelling properties must have an extremely high mass sensitivity. Techniques based on the use of a quartz crystal microbalance (QCM) have the required sensitivity and are well-suited for studies of swelling in very thin films.<sup>7</sup> The quartz crystal microbalance consists of a quartz crystal sandwiched between two metal electrodes. Applying an alternating electric potential across the crystal induces vibrational motion of the crystal. These vibration motions result in a transverse acoustic shear wave which propagates through the crystal. When a thin film is deposited on the top of the crystal, the transverse

acoustic wave propagates through the crystal, the interface, and the foreign layer, thereby changing the resonant frequency of the system. If certain conditions are met, the change in the resonant frequency can be directly related to the mass of the film which rests on the electrode surface. Unfortunately, many factors can complicate this analysis, including viscoelastic energy dissipation within the thin film, interfacial slippage, or a nonuniform mass distribution.<sup>8–11</sup> In these cases additional information can be obtained from the shape of the resonance, although the analysis is not necessarily straightforward.<sup>12–14</sup>

Because the QCM can be sensitive to the mechanical properties of a thin film in ways that are difficult to quantify, it is often essential to have a more direct method for determining the film thickness (or total mass). A variety of techniques can be used to more directly measure the swelling of thin polymer films, including X-ray or neutron reflectivity<sup>15</sup> or ellipsometry. Ellipsometry is very sensitive to both the thickness and the refractive index of a thin film.<sup>16</sup> This technique has been applied to study a variety of features of polymer thin films, including swelling by small molecule solvents,<sup>17–20</sup> and thickness effects on the glass transition.<sup>21–23</sup> In the work described in this paper, we use QCM analysis and ellipsometry as complementary techniques to study the swelling behaviors of hydrophilic polymers and hydrophilic–hydrophobic block copolymers in humid environments and in water. By using impedance spectroscopy, we show that the swelling curves obtained from the two methods are in reasonable agreement when the shape of the quartz crystal resonance in frequency space is not affected by the water content of the films.

\* To whom correspondence should be addressed.

<sup>†</sup> Department of Chemical Engineering.

<sup>‡</sup> Department of Materials Science and Engineering.

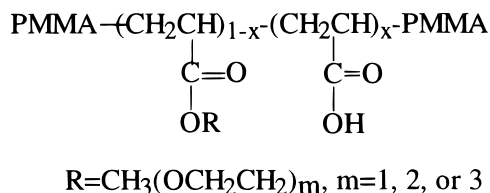


**Figure 1.** Triblock copolymers which have been synthesized and used in this paper. The polymers have  $m = 1$ , poly(methoxymonoethylene glycol acrylate) (P(MMGA-*r*-AA)),  $m = 2$ , poly(methoxydiethylene glycol acrylate) (P(MDGA-*r*-AA)), or  $m = 3$ , poly(methoxytriethylene glycol acrylate) (P(MTGA-*r*-AA)). Random copolymers with composition corresponding to the midblocks of these polymers have also been studied.

The basic hydrophilic copolymer used in our experiments is an acrylic polymer with very short poly(ethylene glycol) (PEG) side chains. To prevent the dissolution of these hydrophilic polymers in water, we have synthesized a variety of block copolymers consisting of poly(methyl methacrylate) (PMMA) hydrophobic anchoring blocks which are coupled to the water-soluble PEG-acrylate blocks. The synthesis and detailed characterization of these polymers are described in another publication.<sup>24</sup> Our focus here is on the swelling behavior of these polymers as obtained by QCM experiments and by ellipsometry.

## Experimental Section

**Materials.** Hydrophilic PEG-acrylates were synthesized by transesterification of anionically polymerized poly(*tert*-butyl acrylate) (PtBA). A detailed description of their synthesis and characterization is given elsewhere.<sup>24</sup> Briefly, the procedure is an adaptation of the method described by Varshney et al. for the synthesis of poly(*n*-butyl acrylate) and PMMA-poly(*n*-butyl acrylate) block copolymers.<sup>25</sup> Instead of using butanol during the acid-catalyzed conversion of the poly(*tert*-butyl acrylate), we used alcohols which can be viewed as monomethoxy-terminated poly(ethylene glycols) with degrees of polymerization of 1, 2, or 3. The resulting repeat polymeric repeat units are referred to as methoxymonoethylene glycol acrylate (MMGA) for  $m = 1$ , methoxydiethylene glycol acrylate (MDGA) for  $m = 2$ , and methoxytriethylene glycol acrylate (MTGA) for  $m = 3$ . Because acrylic acid groups are also introduced during the conversion reaction, polymers produced from a PtBA homopolymer are actually copolymers consisting of PEG-acrylate repeat units and acrylic acid repeat units. While the distribution of these acrylic acid groups along the polymer molecules is unknown, we expect that the distribution is nearly random. We therefore refer to these copolymers as random copolymers. These polymers have a monodisperse distribution of backbone chain lengths but are polydisperse in their composition because of the nature of the conversion process. Hydrophilic/hydrophobic block polymers of the sort shown in Figure 1 were synthesized by using PMMA-PtBA-PMMA triblock copolymers as the base polymers for the conversion reactions. We refer to these polymers simply as "triblock copolymers", even though the midblocks are themselves random copolymers of acrylic acid and a PEG-acrylate.

Number average degrees of polymerization for the random polymers were obtained from size exclusion chromatography (SEC) of the PtBA homopolymer precursor. Degrees of polymerization for triblock copolymer midblocks were obtained from SEC analysis of a PtBA sample which was removed from the polymerization flask prior to the addition of methyl methacrylate monomer. Relative PMMA and PtBA block lengths were determined by <sup>1</sup>H NMR, as were the acrylic acid contents of the converted polymers. The characteristics of the polymers used in these experiments are summarized in Table 1.

**Quartz Crystal Microbalance Measurements.** The experimental setup for the quartz crystal microbalance experiments is shown schematically in Figure 2. The circular, 5.0

MHz AT-cut quartz crystal resonators (International Crystal Manufacturing Co. Inc.) had diameters of 1.37 cm. Circular electrodes on either side of the crystals had diameters of 0.95 cm. The crystals were rinsed with acetone and dried with a strong stream of pure nitrogen prior to use. After measuring the resonant frequency of a clean crystal, a polymer film was deposited on one side of the resonator by spin casting from solutions in methanol (for the random copolymers), mixtures of ethanol and toluene (for the PEG-acrylate block copolymers), or *N,N*-dimethylformamide (for the acrylic acid block copolymer). The humidity in the sample chamber was controlled with saturated inorganic salt solutions.<sup>26</sup> Resonant frequencies were determined by a laboratory crystal oscillator (International Crystal Manufacturing Co. Inc.) and were measured at intervals of 1 s during an experiment. All measurements were done at room temperature. For the dynamic scan in water, the quartz crystal was placed between two O-rings in a liquid flow cell (Universal Sensors, Inc.). In this case the coated electrode surface was exposed to water, and the bare electrode surface was exposed to air. Time-dependent data were obtained as water was added to the flow cell.

**Impedance Spectroscopy.** Admittance measurements were performed with a computer-controlled Schlumberger 1260 frequency response analyzer with Z60 data collection software (Scribner Associates) with an output voltage of 1 V over a frequency range from 4.99 to 5.01 MHz. Quartz crystals exposed to various humidities were connected directly to the impedance analyzer with a two-point electrode configuration.

**Ellipsometry.** Ellipsometry spectra were obtained using a spectroscopic ellipsometer (J.A. Woollam Co., Inc.) fitted with a specially designed sample cell. The humidity in the sample cell, shown in Figure 3, was maintained by saturated salt solutions. The cell has windows fixed at angles of 74.5° from the normal to the sample. We typically obtained data over wavelengths ranging from 400 to 800 nm. Data were analyzed to obtain best-fit film thicknesses and refractive indices using a Levenberg-Marquardt algorithm.<sup>27</sup> A similar ellipsometry cell was used to immerse thin film samples in water during experiments.

## Results and Discussion

**Swelling Behavior of PEG-Acrylate/Acrylic Acid Random Copolymers.** We begin here by describing results obtained from the quartz crystal microbalance (QCM) for swelling of the random copolymers. Representative data are shown in Figure 4. Here we plot changes in the resonant frequency,  $f$ , of the quartz crystal induced by changes in the humidity. The reference frequency,  $f_{\text{dry}}$ , corresponds to the resonant frequency for a completely dry film, in equilibrium with zero relative humidity. The resonant frequency decreases while the polymer absorbs water vapor and increases while water is desorbed from the polymer. If the film is uniform and sufficiently thin, is rigidly coupled to the quartz crystal, and has the appropriate mechanical properties, then the Sauerbrey equation can be used to relate the frequency shift,  $\Delta f$ , to a mass change  $\Delta m$ :<sup>28</sup>

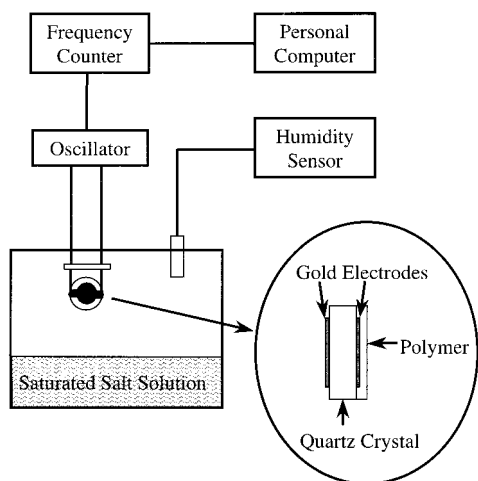
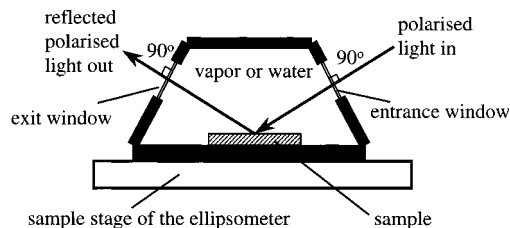
$$\Delta f = f - f_{\text{dry}} = -2f_0^2 \Delta m / A(\mu_q \rho_q)^{1/2} = -C_f \Delta m / A \quad (1)$$

Here  $f_0$  is the resonant frequency of the quartz crystal (5 MHz),  $A$  is the electrode area (0.71 cm<sup>2</sup>),  $\mu_q$  is the shear modulus of the quartz ( $2.95 \times 10^{11}$  dyn cm<sup>-2</sup>),  $\rho_q$  is the density of quartz (2.65 g/cm<sup>3</sup>), and  $C_f$  is the integral sensitivity constant. For these values of  $f_0$ ,  $A$ ,  $\mu_q$ , and  $\rho_q$ ,  $C_f$  is equal to 0.057 Hz cm<sup>2</sup>/ng. The resonant frequency can easily be measured to within 1 Hz with standard electronics, so the sensitivity of our device is approximately 12 ng, which over the electrode area of 0.71 cm<sup>2</sup> corresponds to a water layer with a thickness

**Table 1. Characterization of the Polymers Used in These Experiments**

no.	polymer	$N^a$	$M_w/M_n^b$	$x^c$	$w^d$
1	PMMA	5000	1.09	0	0
2	P(MMGA- <i>r</i> -AA)	547	1.41	0.20	0.08
3	P(MDGA- <i>r</i> -AA)	469	1.39	0.43	0.17
4	P(MTGA- <i>r</i> -AA)	398	1.04	0.46	0.16
5	PMMA-P(MTGA- <i>r</i> -AA)-PMMA	90-363-90	1.19		
6	PMMA-P(MTGA- <i>r</i> -AA)-PMMA	150-336-150	1.18	0.52	0.19
7	PMMA-P(MTGA- <i>r</i> -AA)-PMMA	220-664-220	1.27	0.48	0.17
8	PMMA-PAA-PMMA	220-664-220	1.27	1.00	1.00
9	PMMA-PnBA-PMMA	220-664-220	1.27	~0	~0

<sup>a</sup> Degree of polymerization. <sup>b</sup> Polydispersity index. <sup>c</sup> Mole fraction of acrylic acid groups (not including the PMMA blocks for the block copolymers). <sup>d</sup> Weight fraction of acrylic acid groups, obtained from  $x$  by accounting for the molecular weights of the repeat units: 48 g/mol for AA, 130 g/mol for MMGA, 174 g/mol for MDGA, and 218 g/mol for MTGA.

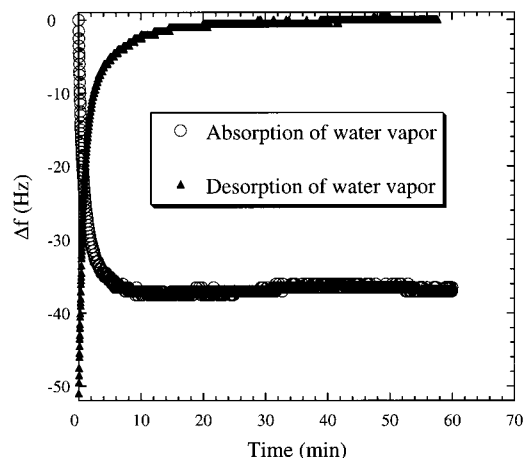
**Figure 2.** Schematic representation of the quartz crystal microbalance.**Figure 3.** Schematic diagram of the sample cell for the ellipsometric measurements. Humidity was controlled by using inorganic salt solutions. Immersion experiments were conducted by filling the cell with water.

of 0.2 nm. Alternatively, the device is sensitive to the addition of 0.2% water to polymer film with a thickness of 100 nm.

The first step in obtaining a swelling curve from the quartz crystal microbalance is to measure  $f_0$ , the resonant frequency of the bare crystal at a humidity of zero. The polymer film of interest is then cast onto the quartz crystal, and  $f_{dry}$  is obtained as the resonant frequency for a relative humidity of zero. For situations where the resonant frequency is indeed proportional to the mass of the thin film, swelling curves can be obtained from subsequent measurements of the resonant frequency,  $f$ , at different humidities, according to the following expression:

$$\phi_{w/w} = \frac{f - f_{dry}}{f - f_0} \quad (2)$$

where  $\phi_{w/w}$  is the weight fraction of water in the films. Overall film thicknesses in our case are typically

**Figure 4.** Representative frequency shifts during absorption and desorption of water from a polymer film as obtained from the quartz crystal microbalance.

between 50 and 150 nm. When the water absorption of the films is low, as with PMMA homopolymers, it is important to correct for frequency changes due to the adsorption of water onto the uncoated surface of the crystal. Equation 2 is valid whenever the resonant frequency is a simple linear function of the mass of the film. In other words,  $C_f$  must be independent of the water content of the films in order for this expression to be valid.

Swelling curves obtained from the quartz crystal microbalance for the random copolymers are shown in Figure 5. Note that the data are plotted as a relative frequency shift and not as an actual weight fraction of water. We plot the data this way because the conditions required for eq 2 to be applicable are not always met in our experiments. However, as discussed in more detail below, we believe that eq 2 is indeed applicable for these films, so that the relative frequency shifts plotted in Figure 5 are equivalent to the weight fraction of water in the polymer films. The random copolymers with the longest PEG side groups ( $m = 3$ ) absorb the most water, and those with the shortest PEG side groups ( $m = 1$ ) absorb the least. The swelling curve for the P(MTGA-*r*-AA) random polymer ( $m = 3$ ) is very similar to the swelling curve for a low molecular weight dimethoxy-terminated poly(ethylene glycol).<sup>29</sup>

Because of concerns about the applicability of the Sauerbrey equation for films studied in our experiments, we have also obtained swelling curves from spectroscopic ellipsometry. The ellipsometric angles ( $\Psi$  and  $\Delta$ ) for a P(MTGA-*r*-AA) polymer on a silicon wafer are shown in Figure 6 for a range of humidities. As the humidity is increased, the maximum in  $\Psi$  and the



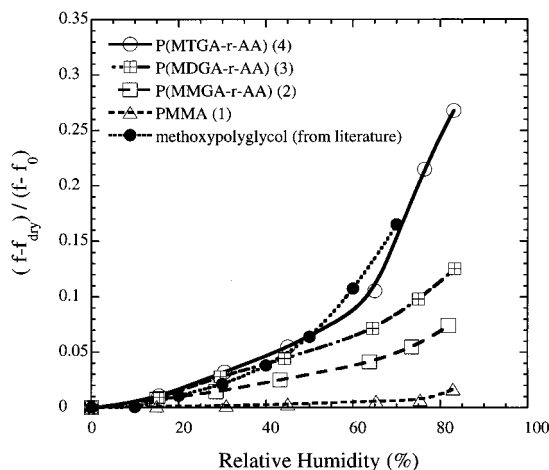


**Figure 5.** Relative frequency shifts from the quartz crystal microbalance for different PEG-acrylates as a function of relative humidity. Numbers in parentheses correspond to the different polymers listed in Table 1.

minimum in  $\Delta$  both shift to longer wavelengths. These data were fit to a model consisting of a uniform single layer in which the dispersion of the refractive index is described analytically as

$$n(\lambda) = n_0 + C_1/\lambda^2 + C_2/\lambda^4 \quad (3)$$

where  $\lambda$  is the wavelength of light, and  $n_0$ ,  $C_1$ , and  $C_2$  are constants obtained by data fitting. The refractive index and thickness of the film are determined independently. The refractive index of a water-swollen polymer,  $n$  (at a given wavelength), can be expressed as a function of the volume fraction of water in the polymer,  $\phi_{v/v}$ , making use of an effective medium approximation derived from the Lorentz–Lorenz equation:<sup>30</sup>

$$\frac{n^2 - n_{\text{pol}}^2}{n^2 + 2n_{\text{pol}}^2} = \phi_{v/v} \frac{n_{\text{water}}^2 - n_{\text{pol}}^2}{n_{\text{water}}^2 + 2n_{\text{pol}}^2} \quad (4)$$

where  $n_{\text{water}}$  is the refractive index of water (1.333 when  $\lambda = 500$  nm) and  $n_{\text{pol}}$  is the refractive index of the dry polymer at the same wavelength. The volume fraction of water in the films can be obtained directly from ellipsometric thickness according to the following expression:

$$\phi_{v/v} = (h - h_{\text{dry}})/h \quad (5)$$

where  $h$  is the measured film thickness, and  $h_{\text{dry}}$  is the value of  $h$  when the relative humidity is equal to zero. Figure 7 shows swelling data (both thickness and refractive index at 500 nm) for the P(MTGA-*r*-AA) polymer. The dashed line represents the prediction of eq 4 with  $\phi_{v/v}$  given by eq 5 and  $n_{\text{pol}}$  set at the experimentally determined value of 1.512. Note the excellent agreement between these values and the values obtained by letting the refractive index float as a free parameter. This agreement gives us great confidence in the interpretation of the results from ellipsometry.

At this point we are in a position to compare the swelling curves obtained from ellipsometry to those obtained from the quartz crystal microbalance. Qualitatively, the curves are very similar, as one can see by comparing the data for the P(MTGA-*r*-AA) polymer plotted in Figures 5 and 7. Quantitative agreement

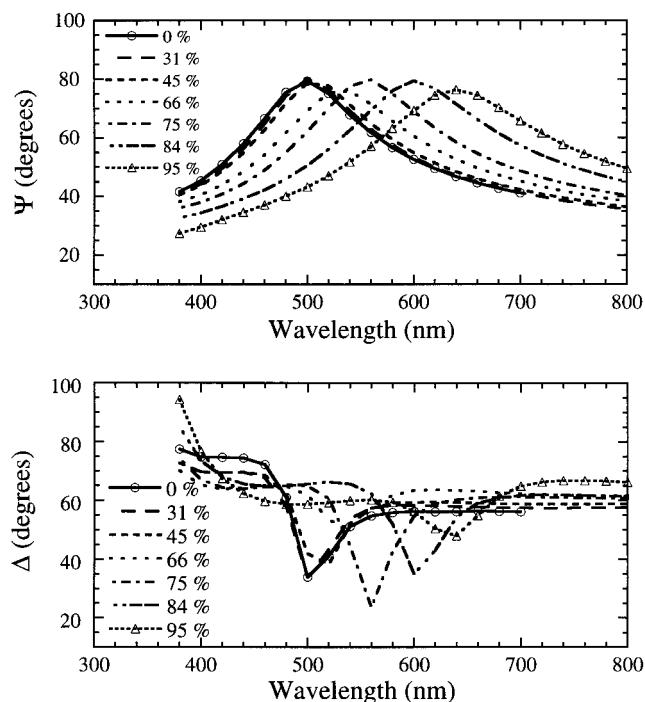


**Figure 6.** Ellipsometric angles  $\Psi$  and  $\Delta$  as a function of wavelength for a series of humidities for P(MTGA-*r*-AA).

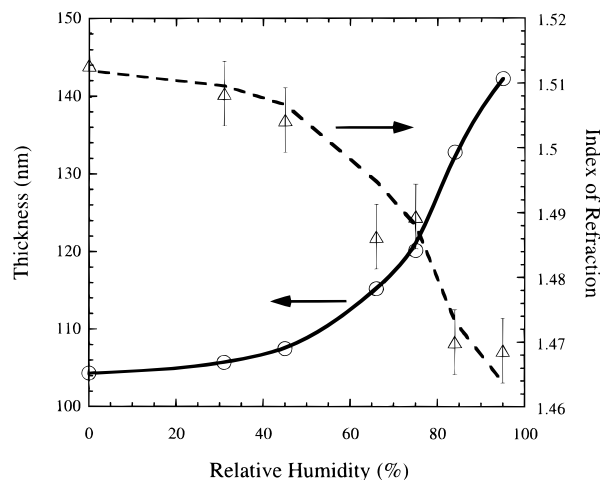


**Figure 7.** Ellipsometric thickness and index of refraction of P(MTGA-*r*-AA) as a function of humidity. The dashed line is the refractive index as predicted by eq 4, with  $n_{\text{polymer}} = 1.512$ ,  $n_{\text{water}} = 1.333$ , and  $\phi_{v/v}$  determined from the measured thickness values.

between these two figures is also quite satisfactory. This quantitative comparison is more clearly illustrated in Figure 13, where the swelling curves are shown in the same figure. Our assumption here is that the density of the random copolymers is close to that of water, so that the weight fractions obtained from the QCM measurements and the volume fractions obtained from ellipsometry can be compared. The similarity between the swelling curves obtained from the two methods is encouraging and indicates that for these polymers the shift in resonant frequency is indeed proportional to the total mass of the film, with a proportionality constant that does not depend on the water content. This result is consistent with more detailed results obtained from impedance spectroscopy, as described in more detail below.

**Swelling Behavior of Block Copolymers: QCM Measurements.** Contrary to the results obtained from

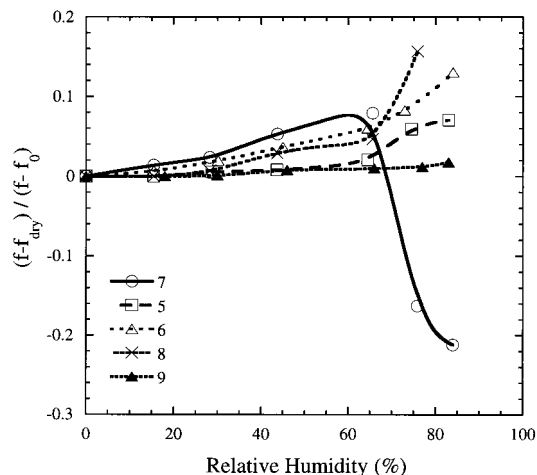


**Figure 8.** Relative frequency shifts from the quartz crystal microbalance for different block copolymers listed in Table 1 as a function of relative humidity.

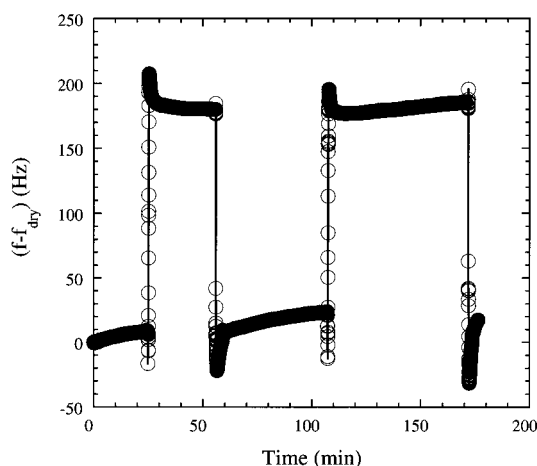


**Figure 9.** Frequency shifts obtained from the QCM for a PMMA-P(MTGA-*r*-AA)-PMMA triblock copolymer (no. 7) during humidity cycling between 0% RH ( $\Delta f \approx 0$ ) and 84% RH ( $\Delta f \approx 180$  Hz).

the homopolymers, a straightforward interpretation of the QCM results is not generally possible for the block copolymers. Figure 8 shows the relative frequency shift for a series of triblock copolymers as a function of humidity. Each of the triblock copolymers has PMMA end blocks and a converted form of PtBA as the midblock. Several different compositions of the midblock were studied, including poly(acrylic acid) (PAA), poly(*n*-butyl acrylate) (PnBA), and P(MTGA-*r*-AA) with a composition similar to the random copolymer described in the previous section. In most cases, the relative frequency shifts look qualitatively similar to those obtained for the random copolymers. However, for humidities above 75%, the resonant frequency for sample 7 unexpectedly increases with increasing humidity. Clearly eq 1 is not valid here, since this would imply an inverse relationship between the humidity and the water content of the films.

To test the reproducibility of our result, we cycled the film between humidities of zero and 84% while monitoring the resonant frequency of the quartz crystal. The results of this experiment for triblock copolymer 7 are plotted in Figure 9. After equilibration at zero humidity, the humidity was abruptly changed to 84% at a time of 25 min by moving the crystal to a different environmental chamber. The resonant frequency initially de-

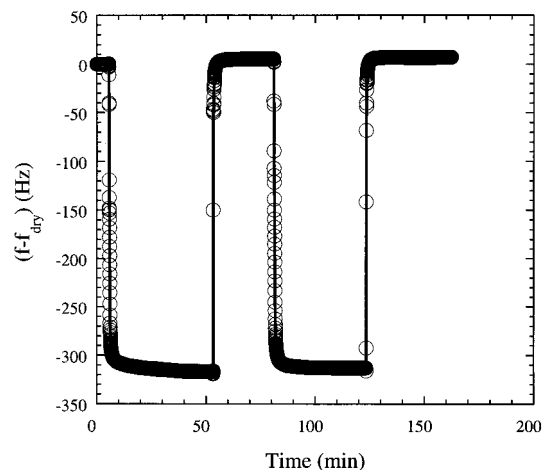


**Figure 10.** Frequency shifts obtained from the QCM for P(MTGA-*r*-AA) during humidity cycling between 0% RH ( $\Delta f \approx 0$ ) and 84% RH ( $\Delta f \approx -320$  Hz).

creases as the film begins to absorb water, but this decrease is overwhelmed by an unexpected, rapid increase in the frequency of about 230 Hz. The frequency then continues to decrease until it reaches a characteristic plateau. The reverse behavior is observed when the humidity is changed back to zero at a time of 55 min. Here a relatively small increase in the resonant frequency is superposed on an extremely rapid 230 Hz decrease in the frequency. These general features are observed again as the humidity is changed to 84% at 108 min and to zero at 171 min. These results can be compared to the response of a P(MTGA-*r*-AA) random copolymer which is plotted in Figure 10. Here the resonant frequency rapidly adjusts to a single new value when the relative humidity (RH) is changed. Deviations of the response from a perfect square wave can be attributed to the time required for equilibration of the humidity as the QCM is moved between different environmental chambers. Equilibration in situations where the humidity is increased (decreasing resonant frequency) is somewhat slower than for cases where the film is cycled between 0% RH and 84% RH.

The behavior illustrated by the polymers in Figures 9 and 10 is actually similar in some important respects. In both instances there is a contribution to the resonant frequency that decreases as the humidity increases. For triblock copolymer 7, there is an additional contribution to the resonant frequency that is not present for the other polymers. This additional contribution can be treated as an offset to the resonant frequency which is essentially a step function. For humidities larger than approximately 70%, this offset is 230 Hz, whereas it is essentially zero for humidities less than 70%. If one subtracts 230 Hz from  $f$  and uses this adjusted value in eq 2, one obtains 0.08 for  $\phi_{w/w}$  for the triblock copolymer at a humidity of 84%. While this value is still less than the volume fraction of water obtained from ellipsometry, it is at least consistent with the values obtained from the QCM measurements at lower values of the humidity.

While it is not possible to predict quantitatively the magnitude of the 230 Hz frequency shift shown in Figure 9, it is clear that the origins of this frequency shift relate to changes in the mechanical response of the triblock copolymer as the humidity is increased. Additional information is obtained from the impedance spectra. For our purposes it is convenient to work in

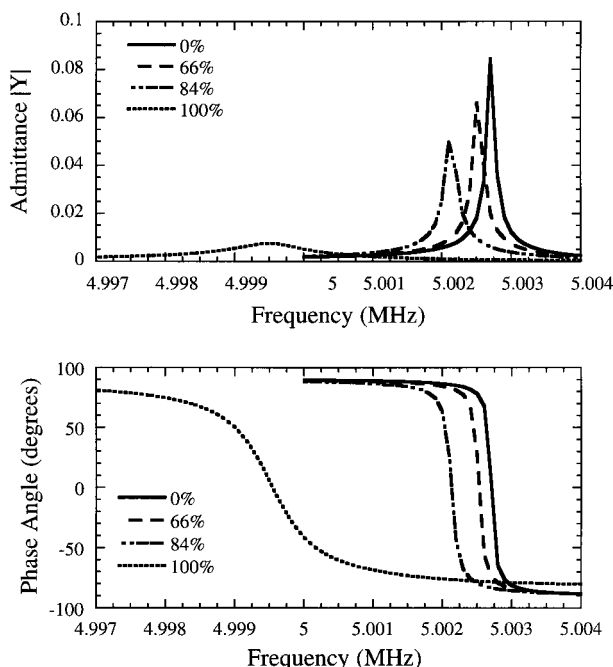


**Figure 11.** Impedance response for P(MTGA-*r*-AA) at different humidities: (top) admittance amplitude vs frequency, (bottom) phase angle vs frequency.

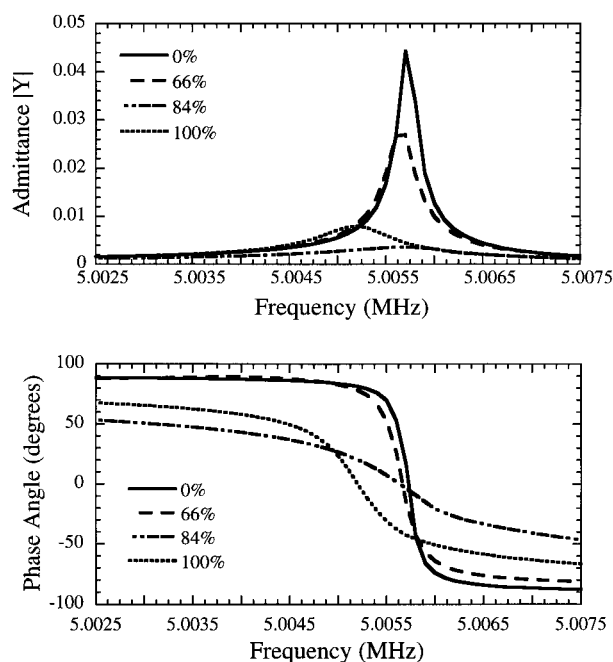


**Figure 12.** Impedance response for a PMMA-P(MTGA-*r*-AA)-PMMA triblock copolymer (no. 7) at different humidities: (top) admittance amplitude vs frequency, (bottom) phase angle vs frequency.

terms of the admittance (the inverse of the impedance), defined as the ratio of the ac current across the quartz crystal to the input ac voltage. As the admittance is a complex quantity, it has a magnitude,  $|Y|$ , and a phase angle. These quantities are plotted as a function of frequency for a random copolymer at different humidities in Figure 11 and for a triblock copolymer in Figure 12. Away from resonance, the quartz crystal acts as a simple capacitor, and the phase angle is equal to  $90^\circ$ . The phase angle passes through zero at the resonance, where the admittance amplitude reaches a maximum. The quality factor for the oscillator is described by the width of the resonance and is a measure of energy

dissipation. Viscoelastic energy dissipation in the polymer film decreases the quality factor of the resonator, increasing the width of the resonance. The phase angle returns to  $90^\circ$  beyond the antiresonance, where the admittance amplitude goes through a minimum. The antiresonant frequency is about 10 kHz higher than the resonant frequency, as has been observed previously.<sup>11,31</sup>

In addition to changing the width of the resonance, dissipative processes also shift the resonant frequency. It is for this reason that application of the Sauerbrey equation is not possible when the viscoelastic properties in the film are changing. Sometimes the effects of mass loading and the effects of viscous dissipation on the resonant frequency are separable, so that reasonable values for mass loading can still be obtained from simple measurements of the resonant frequency.<sup>32</sup> When a quartz crystal microbalance is immersed in water, for example, there is an immediate decrease in the resonant frequency which is accompanied by a broadening of the resonance. Subsequent increases in the mass associated with absorption to the QCM electrode surface from water can then be described by the Sauerbrey equation, provided that the adsorbed species is rigidly coupled to the electrode surface and that the viscoelastic properties of the overall layer on the electrode surface remain constant.<sup>33</sup> We use the width of the resonance as an empirical measure of the potential importance of viscoelastic energy dissipation. If the width of the resonance is constant, then we believe that swelling curves based on the Sauerbrey equation are likely to be valid. Plots of the frequency dependence of the phase angle are quite helpful in this sense. If two peaks have the same shape, plots of their phase angles will be identical, apart from a horizontal shift equal to the change in resonant frequency. As shown in Figure 11, the peak shapes are indeed identical for the random copolymers for relative humidities up to 84%. As discussed previously, swelling curves obtained from the QCM and from ellipsometry are in good agreement for these polymers. Agreement between swelling curves obtained by the two methods for the triblock copolymers is much less satisfactory, as one would expect from the different shapes of the resonance curves shown in Figure 12. Our conclusion with regard to the swelling curves is that accurate data can be obtained by application of the Sauerbrey equation, provided that the shapes of the curves do not depend on the solvent volume fraction. Similar conclusions with regard to the applicability of the Sauerbrey equation have been demonstrated previously by others.<sup>13,34</sup>

Our interpretation of the results shown in Figure 9 is that the large frequency shift is indicative of a phase transition in the polymer film. Very recently, Teuscher et al. have demonstrated that phase transitions in *n*-alkanes can be distinguished by measuring the resonant frequency in addition to the peak admittance amplitude.<sup>32</sup> As illustrated in Figure 12, the transition in our film (with increasing humidity) is accompanied by an increase in the resonant frequency and by a substantial decrease in the peak admittance amplitude. A similar signature has been observed by Teuscher et al. for a solid/solid phase transition in *n*-alkanes. While not the central focus of this paper, the ability to observe phase transitions in block copolymer films with thicknesses of 100 nm (or less) is an exciting development. It is well-known, for example, that the structures of block copolymer materials are highly dependent on the processing conditions.<sup>35</sup> Certainly the spun-cast films

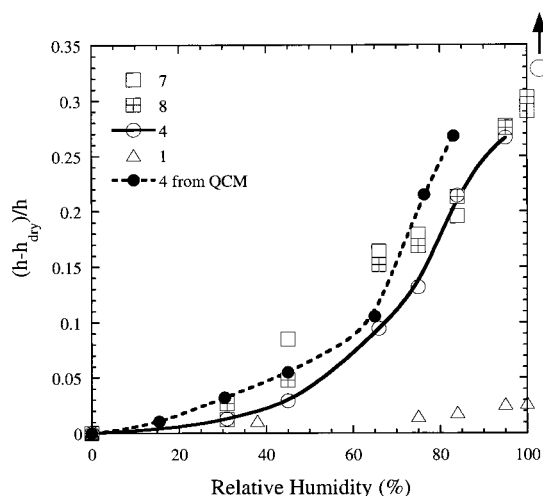


**Figure 13.** Ellipsometrically determined swelling curves. The solid and dashed lines illustrate the comparison between swelling curves obtained by ellipsometry and QCM measurements for the P(MTGA-*r*-AA) random copolymer.

used in our experiments cannot be assumed to be fully equilibrated. Indeed, a film of the same triblock copolymer produced by dip coating did not show any evidence for a phase transition, even though Figure 9 shows that the results described above from the spun-cast film were quite repeatable. The ability to use these types of measurements to probe the effects of processing conditions on the structure of very thin block copolymer films is potentially very useful.

An additional explanation for the large frequency jumps shown in Figure 9 that must also be considered involves a film resonance, which occurs when the acoustic wavelength in the film is equal to 4 times the film thickness. If this condition is met, the frequency shift reverses sign, and the width of the resonance is very large.<sup>36</sup> While this result is qualitatively consistent with our observations, the thickness of our films ( $\sim 100$  nm) is a factor of 100 less than the estimated required thickness for the occurrence of the film resonance.<sup>12</sup> This estimate corresponds to materials with similar viscoelastic properties to ours. For this reason, we believe the existence of a humidity-induced phase transition is the most likely explanation for the results we have observed. Unfortunately, we do not have a firm explanation for the origins of this phase transition. One possibility is that increasing the water content disrupts interactions between acrylic acid groups and the ether linkages of the PEG side chains. These interactions are known to be important in concentrated polymer solutions<sup>37</sup> and may play a role in our systems as well.

**Swelling Behavior of Block Copolymers: Ellipsometric Measurements.** Because of the complications mentioned above, use of a more direct technique such as ellipsometry is essential in order to obtain accurate swelling curves for the triblock copolymers. Swelling curves, determined by ellipsometry, for triblock copolymers with P(MTGA-*r*-AA) and poly(acrylic acid) midblocks are shown in Figure 13. Swelling curves for a P(MTGA-*r*-AA) random copolymer and for a PMMA homopolymer are included for comparison. Note that for humidities between 35% and 80% both triblock copolymers swell more than the random copolymers that comprise the midblocks. While we do not have a clear explanation for this result at this point, it may be attributable to compositional differences between the

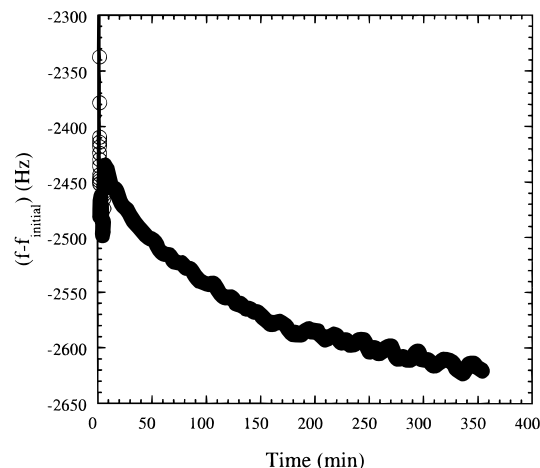


**Figure 14.** Time dependence of the QCM frequency response after immersion of a PMMA-P(MTGA-*r*-AA)-PMMA triblock copolymer (no. 7) in water. The frequency is referenced to the value for the dry film, before immersion in water.

different polymers. The important result is that the addition of the PMMA end blocks stabilizes the films so that they do not dissolve in water or dewet from the substrate, while not decreasing the water uptake. This result is the expected one if the block copolymers form a microphase-separated morphology where the midblocks span a matrix of nearly pure P(MTGA-*r*-AA), while the PMMA blocks segregate into spherical domains which act as physical cross-links. As described in the Appendix, the concentration of elastically effective strands, corresponding to hydrophilic midblocks bridging the PMMA domains, is simply too low to contribute substantially to the deformation free energy for solvent volume fractions less than about 0.5. This elastic free energy dominates the behavior at very high solvent volume fractions, however, so that the block copolymers are not able to dissolve completely. Our assumption here is that the random copolymer midblocks are immiscible with the PMMA end blocks. This assumption is consistent with the measured glass transition temperatures of the block copolymers and of corresponding blends.<sup>24</sup>

**Dynamic Swelling Behavior of Block Copolymers in Water.** To characterize more completely the behavior of the films in aqueous environments, we also conducted experiments where the polymers were completely immersed in water. For the QCM measurements, we equilibrated the dry polymer film in room humidity (32%) and then added water to the liquid flow cell. The resonant frequency immediately decreased by about 2000 Hz as shown in Figure 14. The resonant frequency fluctuated over the next few minutes before slowly decaying over a time scale of several hours. To separate film thickness effects from changes in the mechanical properties of the thin film, ellipsometric measurements were also conducted. The time dependence of the ellipsometric thickness and of the refractive index is shown in Figure 15. The refractive index and thickness are in agreement with each other, according to the prediction of eq 4, with  $n_{\text{polymer}} = 1.486$ . The thickness reaches a plateau corresponding to  $\phi_{v/v} = 0.46$  after about 2 h, whereas the properties of the film probed by the quartz crystal microbalance continue to change after 6 h. These changes are much slower than what would be expected simply from diffusion of water into the polymer films. The diffusion coefficient of water in amorphous poly(ethylene oxide), which should be comparable to the



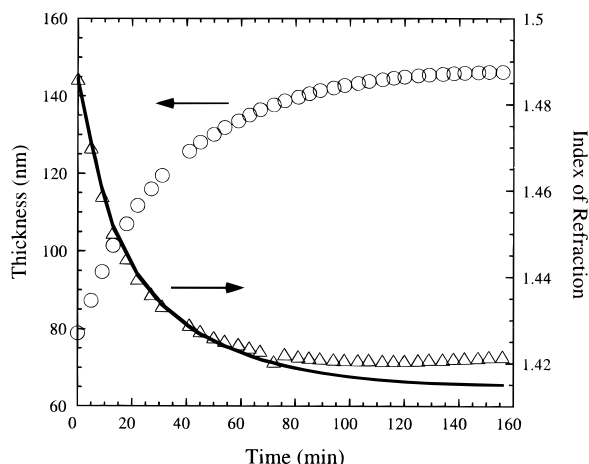


**Figure 15.** Time dependence of the ellipsometric thickness and index of refraction for a PMMA-P(MTGA-*r*-AA)-PMMA triblock copolymer (no. 7) after immersion in water.

coefficient in our polymers, is about  $2 \times 10^{-6} \text{ cm}^2/\text{s}$ .<sup>38</sup> The corresponding time for water to diffuse through the entire thickness of our films is much less than a millisecond, so the swelling process is clearly not diffusion limited. In addition, the final volume fraction of water obtained by immersion of the samples is 0.46, whereas the equilibrium volume fraction of water for samples that are exposed to air at a relative humidity of 100% is only 0.30.

Our interpretation of these results is that the long relaxation times observed for the immersion experiments represent the response of the material to osmotic swelling stresses. Mechanical relaxations in response to these stresses allow additional solvent to be incorporated into the film. The quartz crystal microbalance is sensitive to mechanical properties of the block copolymer film which continue to evolve with time, even after the thickness of the film is no longer changing. Because the block copolymer films do not dissolve in water, and adhere reasonably well to a variety of materials, they are excellent candidates for surface modification when a hydrophilic surface is desired.

## Summary

Two complementary methods, the quartz crystal microbalance and spectroscopic ellipsometry, have been used to characterize the swelling of hydrophilic polyacrylates by water vapor and bulk water. Agreement between swelling curves obtained from the two methods is good, provided that the shape of the QCM resonance is not affected by the water content of the films. We find that plots of the frequency dependence of the phase angle provide a very convenient method for comparing peak shapes. Random copolymers of poly(acrylic acid) and PEG-acrylates show an increasingly favorable interaction with water as the degree of polymerization,  $m$ , of the PEG side chains increases from one to three. The solubility properties of a polymer with  $m = 3$  and 16 wt % acrylic acid are very similar to the solubility properties of low molecular weight dimethoxy-terminated poly(ethylene glycol). Addition of PMMA end blocks to this polymer to make a triblock copolymer does not reduce the equilibrium swelling for relative humidities less than 80%. The end blocks do stabilize the polymer coating, however, so that it does not dissolve when immersed in water. For this reason we are able to track the time dependence of the properties of a

triblock copolymer film after immersion in water, finding that these properties continue to change even after the film thickness as determined by ellipsometry has stabilized. Finally, we have presented evidence for the existence of a reversible phase transition in a triblock copolymer film that can easily be detected by the quartz crystal microbalance.

**Acknowledgment.** Work conducted at Northwestern University was supported by the MRSEC program of the National Science Foundation (DMR-9632472) at the Materials Research Center of Northwestern University. The UK Engineering and Physical Sciences Research Council provided funding for D.A.S. and for the purchase of the ellipsometer. Work done at the University of Surrey was generously supported by Zeneca plc through their Strategic Research Fund. Helpful discussions with Dr. S. Ford and Dr. N. Prokopyuk are gratefully acknowledged, as is the use of the impedance spectrometer provided by Prof. T. Mason.

## Appendix. Swelling Equilibria for Thin Cross-Linked Layers

The structure of a network influences its elastic properties and equilibrium swelling behavior. The swelling of networks by a good solvent is predicted by various models.<sup>39,40</sup> For our purposes, it is sufficient to use the simple model proposed long ago by Flory and others.<sup>41</sup> In this model an elastic free energy of deformation is simply added to the mixing free energy. The extensive free energy of an elastically deformed network,  $\Delta F$ , is then given by the following expression:

$$\frac{\Delta F}{k_B T} = \frac{\nu_e}{2} (\lambda_x^2 + \lambda_y^2 + \lambda_z^2 - 3) - \nu_e \ln(\lambda_x \lambda_y \lambda_z) + n_s \ln \phi_s + \chi n_s \phi_p \quad (6)$$

where  $\lambda_i$  is the extension ratio in the  $i$ th direction,  $\nu_e$  is the number of elastically effective chains,  $\phi_s$  is the solvent volume fraction,  $\phi_p$  is the polymer volume fraction,  $n_s$  is the number of solvent molecules, and  $\chi$  is the polymer/solvent interaction parameter. For a thin film that is laterally confined in the  $xy$  plane,  $\lambda_x = \lambda_y = 1$ ,  $\lambda_z = 1/\phi_p$ , and the free energy can be written in the following form:

$$\frac{\Delta F}{k_B T} = \frac{\nu_e}{2} \left( \frac{1}{\phi_p^2} - 1 \right) + \nu_e \ln(\phi_p) + n_s \ln(1 - \phi_p) + \chi n_s \phi_p \quad (7)$$

The expression for the solvent chemical potential is obtained by differentiating with respect to the number of solvent molecules

$$\mu_s = \left. \frac{\partial \Delta F}{\partial n_s} \right|_{\nu_e} \quad (8)$$

after substituting the following expression for  $\phi_p$ :

$$\phi_p = \frac{\nu_e N}{\nu_e N + n_s} \quad (9)$$

Here  $N$  can be viewed as the average degree of polymerization of an elastically effective strand. More rigorously, it is the ratio of the strand volume to the volume of a solvent molecule. Note that contributions to the polymer volume fraction from elastically ineffective



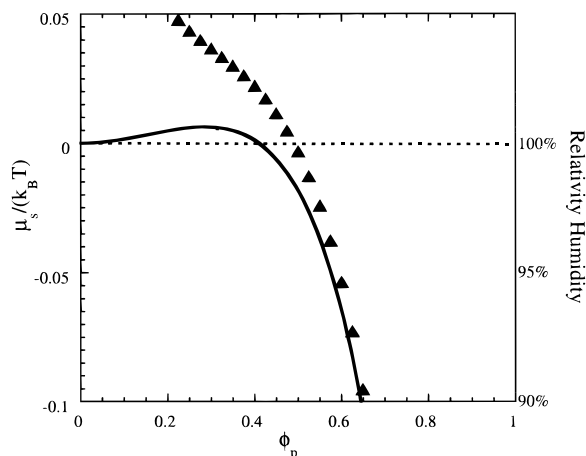


**Figure 16.** Relationship between the solvent chemical potential (or relative humidity) and the polymer volume fraction. Curves have been calculated according to eq 10 for  $\chi = 0.7$  and  $N = \infty$  (solid line) and for  $\chi = 0.7$  and  $N = 100$  (symbols).

“dangling ends” are ignored in this simplified treatment. Effects of hydrogen bonding, which result in a concentration dependence to the effective  $\chi$  parameter,<sup>40,42</sup> have also been ignored.

Evaluation of these expressions gives the following for the solvent chemical potential:

$$\frac{\mu_s}{k_B T} = \frac{1}{\phi_p N} - \frac{\phi_p}{N} + \phi_p + \ln \phi_s + \chi \phi_p^2 \quad (10)$$

The first two terms in eq 10 represent elastic contributions to the chemical potential, and the last three terms represent contributions to the free energy of mixing between a solvent and a melt of un-cross-linked chains with a very high molecular weight.

Equation 10 can be used to explain why the PMMA blocks do not diminish the swelling of the polymers at low humidities, while at the same time preventing these polymers from completely dissolving in water. Figure 16 compares the prediction of eq 10 for  $\chi = 0.7$  and  $N = \infty$  (solid line) to the prediction of this equation for  $\chi = 0.7$  and  $N = 100$  (symbols). The relative humidity (RH) is related to the solvent chemical potential through the following simple expression:

$$\mu_s = k_B T \ln(\text{RH}) \quad (11)$$

Equation 11 has been used to generate a humidity scale which has been added to Figure 16. As the humidity is increased, the solvent chemical potential increases toward zero. The equilibrium composition of the polymer film is determined by the appropriate relationship between the solvent chemical potential and the solvent concentration in the polymer film. The comparison made in Figure 16 shows that the effect of cross-linking on the relationship between the solvent chemical potential and the solvent concentration is minimal for solvent volume fractions less than about 0.4. This comparison is valid for  $N = 100$ , which for water as the solvent corresponds to a molecular weight of only about 2000 g/mol between cross-link points. The physically cross-linked triblock copolymers actually have much higher values of  $N$ , corresponding to the molecular weight of the molecule. Therefore, it is not at all surprising that the swelling of the triblock copolymers is not reduced from the swelling of the random copolymers at low and

intermediate humidities, where the solvent volume fractions are relatively low.

## References and Notes

- (1) Seymour, R. B.; Mark, H. F. *Handbook of Organic Coatings: A Comprehensive Guide for the Coatings Industry*; Elsevier Science Publishing Co., Inc.: New York, 1990.
- (2) *Technology for Waterborne Coatings*; Glass, J. E., Ed.; American Chemical Society: Washington, DC, 1997.
- (3) Desai, N. P.; Hossainy, S. F. A.; Hubbell, J. A. *Biomaterials* **1992**, *13*, 417.
- (4) Walton, D. G.; Soo, P. P.; Mayes, A. M.; Allgor, S. J. S.; Fujii, J. T.; Griffith, L. G.; Ankner, J. F.; Kaiser, H.; Johansson, J.; Smith, G. D.; Barker, J. G.; Satija, S. K. *Macromolecules* **1997**, *30*, 6947.
- (5) López, G. P.; Ratner, B. D.; Tidwell, C. D.; Haycox, C. L.; Rapoza, R. J.; Horbett, T. A. *J. Biomed. Mater. Res.* **1992**, *26*, 415.
- (6) *Hydrophilic Polymers: Performance with Environmental Acceptance*; Glass, J. E., Ed.; American Chemical Society: Washington, DC, 1996.
- (7) An excellent general source of articles describing state of the art applications of the quartz crystal microbalance and related techniques is the recent *Faraday Discussions* volume entitled “Interactions of Acoustic Waves with Thin Films and Interfaces” (*Faraday Discuss.* **1997**, *107*).
- (8) Buttry, D. A.; Ward, M. D. *Chem. Rev.* **1992**, *92*, 1355.
- (9) Ward, M. D.; Buttry, D. A. *Science* **1990**, *249*, 1000.
- (10) Wang, J.; Ward, M. D.; Ebersole, R. C.; Foss, R. P. *Anal. Chem.* **1993**, *65*, 2553.
- (11) Kanazawa, K. K. *Faraday Discuss.* **1997**, *107*, 77.
- (12) Domack, A.; Johannsmann, D. *J. Appl. Phys.* **1996**, *80*, 2599.
- (13) Hillman, A. R. *Solid State Ionics* **1997**, *94*, 151.
- (14) Topart, P. A.; Noël, M. A. M.; Liess, H.-D. *Thin Solid Films* **1994**, *239*, 196.
- (15) Tan, N. C. B.; Wu, W. L.; Wallace, W. E.; Davis, G. T. *J. Polym. Sci., Part B: Polym. Phys.* **1998**, *36*, 155.
- (16) Azzam, R. M. A.; Bashara, N. M. *Ellipsometry and Polarized Light*; North-Holland: Amsterdam, 1977.
- (17) Stromberg, R. R.; Passaglia, E.; Tutas, D. J. *National Bureau of Standards, Miscellaneous Publication* **1963**, *256*, 281.
- (18) Filippov, L. K. *J. Chem. Soc., Faraday Trans.* **1993**, *89*, 4053.
- (19) Kleinfeld, E. R.; Ferguson, G. S. *Chem. Mater.* **1995**, *7*, 2327.
- (20) Tompkins, H. G. *A User's Guide to Ellipsometry*; Academic Press: San Diego, CA, 1993.
- (21) Keddie, J. L.; Jones, R. A. L.; Cory, R. A. *Europhys. Lett.* **1994**, *27*, 59.
- (22) Keddie, J. L.; Jones, R. A. L.; Cory, R. A. *Faraday Discuss.* **1994**, *98*, 219.
- (23) Keddie, J. L.; Jones, R. A. L. *Isr. J. Chem.* **1995**, *35*, 21.
- (24) Chen, W.-L.; Shull, K. R. Manuscript in preparation.
- (25) Varshney, S. K.; Jacobs, C.; Hautekeer, J.-P.; Bayard, P.; Jerome, R.; Fayt, R.; Teyssié, P. *Macromolecules* **1991**, *24*, 4997.
- (26) Ranucci, E.; Ferruti, P. *Macromol. Symp.* **1996**, *109*, 89.
- (27) Marquardt, D. W. *J. Soc. Ind. Appl. Math.* **1963**, *11*, 431.
- (28) Sauerbrey, G. *Z. Phys.* **1959**, *155*, 206.
- (29) Katchman, B.; McLaren, A. D. *J. Am. Chem. Soc.* **1951**, *73*, 2124.
- (30) Born, M.; Wolf, E. *Principles of Optics*; University Press: Cambridge, 1997.
- (31) Yang, M.; Thompson, M. *Langmuir* **1993**, *9*, 802.
- (32) Teuscher, J. H.; Yeager, L. J.; Yoo, H.; Chadwick, J. E.; Garrell, R. L. *Faraday Discuss.* **1997**, *107*, 399.
- (33) Xu, H.; Schlenoff, J. B. *Langmuir* **1994**, *10*, 241.
- (34) Noël, M. A. M.; Topart, P. A. *Anal. Chem.* **1994**, *66*, 484.
- (35) Fredrickson, G. H.; Bates, F. S. *Annu. Rev. Mater. Sci.* **1996**, *26*, 501.
- (36) Domack, A.; Prucker, O.; Rühe, J.; Johannsmann, D. *Phys. Rev. E* **1997**, *56*, 680.
- (37) Tsochida, E.; Abe, K. *Adv. Polym. Sci.* **1982**, *45*, 1.
- (38) *Polymer Handbook*, 3rd ed.; Brandrup, J., Immergut, E. H., Eds.; Wiley: New York, 1989.
- (39) Patel, S. K.; Malone, S.; Cohen, C. *Macromolecules* **1992**, *25*, 5241.
- (40) Painter, P.; Shenoy, S. *Energy Fuels* **1995**, *9*, 364.
- (41) Flory, P. *Principles of Polymer Chemistry*; Cornell University Press: Ithaca, NY, 1953.
- (42) Painter, P. C.; Graf, J. F.; Coleman, M. M. *Macromolecules* **1991**, *24*, 4, 5630.